Journal of Clinical Densitometry: Assessment & Management of Musculoskeletal Health, vol. ■, no. ■, 1–9, 2020

1094-6950/■:1–9/$36.00
https://doi.org/10.1016/j.jocd.2020.10.006

Assessing Periprosthetic Bone in Total Wrist Arthroplasty: The Validity of DXA

Trygve Holm-Glad,[1,2] Kristin Godang,[3] Jens Bollerslev,[2,3] Magne Røkkum,[1,2] and Ole Reigstad[1,2]*

[1] *Division of Orthopaedic Surgery, Oslo University Hospital, Oslo, Norway;* [2] *Institute of Clinical Medicine, University of Oslo, Oslo, Norway; and* [3] *Section of specialized endocrinology, Oslo University hospital, Oslo, Norway*

Abstract

Introduction: Dual-energy X-ray absorptiometry (DXA) can measure bone mineral density (BMD) around joint arthroplasties. DXA has never been used in total wrist arthroplasties (TWA). We investigated (1) whether BMD differs between 2 TWAs implanted in the same cadaver forearm, (2) the effect of forearm rotation and wrist extension on measured BMD around TWA in a cadaver, and (3) the precision of DXA in a cadaver and patients.

Methodology: One ROI around the distal and 1 and 3 ROIs (ROI1-3) around the proximal component were used. Ten DXA scans were performed on forearm and femur mode convertible to orthopedic knee mode without arthroplasty, with ReMotion, and with Motec TWA in one cadaver forearm. Ten scans with 5° increments from 90°−70° pronation and 0°−20° extension, were performed with Motec. Precision was calculated as coefficient of variation (CV%) and least significant change (LSC%) from cadaver scans and double examinations with femur mode converted to orthopedic knee mode in 40 patients (20 ReMotion, 20 Motec).

Results: BMD was higher in all Motec than corresponding ReMotion ROIs ($p < 0.05$). BMD changed with 10° supination in the distal ROI and ROI1, and with 5° extension in the distal ROI ($p < 0.05$). In the cadaver the orthopedic knee mode was more precise than the forearm mode in 3 Motec ROIs ($p < 0.05$). In patients CV was 2.21%−3.08% in the distal ROI, 1.66%−2.01% in the proximal ROI, and 1.98%−2.87% with 3 ROIs.

Conclusions: DXA is feasible for BMD measurement around the proximal component using the orthopedic knee mode, but not the distal component of TWA.

Key Words: Arthroplasty; wrist; DXA; periprosthetic BMD; precision.

Introduction

Total wrist arthroplasties (TWA) have been on the market since the 1970s *(1,2)*. They have not shared the success of total hip arthroplasties and knee arthroplasties with regards to function and survival. Whereas failure and revision rates of earlier TWA were high *(1)*, newer designs reveal more promising mid-term results *(3,4)*.

Following implantation of an arthroplasty the novel load transfer leads to periprosthetic bone remodeling *(5,6)*. Dual-energy X-ray absorptiometry (DXA) can measure bone mineral density (BMD = bone mineral content divided by bone area) around joint arthroplasties *(6)*. BMD becomes higher in areas of implant fixation than areas of stress shielding *(5,6)* and higher around fixed than loose implants *(7,8)*. In addition, wear leading to osteolysis reduces bone mass *(9)*.

Received 05/26/20; Revised 10/12/20; Accepted 10/13/20.
*Address correspondence to: Trygve Holm-Glad, MD, Division of Orthopaedic Surgery, Oslo University Hospital, Oslo, Norway. E-mail: trygve.holm.glad@gmail.com

By dividing the periprosthetic bone into "regions of interest" (ROIs), the BMD can be measured in separate areas around an implant *(5,10)*. Increasing number of ROIs decreases the size of each ROI, leading to lower precision due to a larger impact on BMD from any measurement error *(11)*. As many ROIs as possible with precision high enough to detect clinically relevant BMD changes are desired. Linking a specific BMD loss to implant loosening has been difficult. Thus, the clinically important difference with regards to loosening is unknown.

The DXA software uses an edge detection algorithm to match the tissue density information acquired from the scan with preset density values, thereby separating bone from soft tissue and metal. Software precisely measuring periprosthetic BMD around hip *(12–14)* and knee arthroplasties *(15)* is commercially available, but not for other joints. The knee resembles the wrist more than the hip due to similar bone density and comparable soft tissue thickness. The forearm acquisition mode is not designed for BMD measurement around TWA. DXA has to our knowledge never been used in TWA.

The aim of this study was to evaluate whether BMD differs between 2 arthroplasties implanted in the same cadaver wrist, and the effect of forearm rotation and wrist extension on measured BMD. Furthermore, the precision of BMD analysis around TWA in a cadaver using 2 different acquisition modes, and the precision in patients was investigated.

Materials and Methods

Implants

The ReMotion TWA (Stryker, Inc., Kalamazoo, Michigan, USA) consists of titanium plasmasprayed cobalt chrome (CoCr) stems for uncemented press fit fixation in the radius and capitate, 2 additional CoCr screws for fixation in the carpus, and an ovoid CoCr on polyethylene articulation. The Motec TWA (Swemac Orthopaedics AB, Linköping, Sweden) comprises calcium phosphate coated (Bonit, DOT Medical, Rostock, Germany) grit-blasted titanium alloy stems for uncemented screw fixation in the radius and the capitate/third metacarpal, and a CoCr-on-CoCr ball and socket articulation (Fig. 1).

Cadaver Study

We studied a fresh frozen forearm amputated just distal to the elbow with the entire soft tissue mantle intact, stored at −78°C. The cadaver was thawed at room temperature prior to implant insertion and DXA scans wherein movement of the wrist was required. All other scans were performed with frozen cadaver. The forearm was covered with a thin layer of plastic during the testing. Since thawing can alter the measured BMD *(16)*, the frozen cadaver was scanned 10 times without moving within 1 hour after withdrawal from the freezer, first with forearm mode, then femur mode convertible to orthopedic knee mode (Fig. 2).

Fig. 1. ReMotion (left) and Motec (right) TWA.

After 8 hours thawing, the lunate, proximal two-third of the scaphoid and triquetrum were removed. Medium 30 mm long radial and 19 mm carpal ReMotion stems were inserted using standard operation technique and equipment *(17)*. The specimen was frozen, and 10 scans were performed with forearm and femur mode without moving (Fig. 2).

Following eight hours thawing, the ReMotion implants were exchanged with Motec 38 mm long radial and 50 mm long small metacarpal components, using standard operation technique and equipment *(18)*. Since the ReMotion components are shorter with smaller diameters than Motec, sufficient bone stock had been preserved for implantation of Motec, verified with fluoroscopy. The specimen was frozen and 10 forearm and femur mode scans were performed without moving (Fig. 2). For each

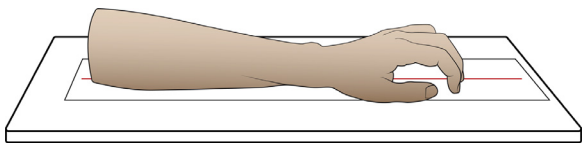

Fig. 2. The forearm rested on two 1.5 cm thick soft tissue density equivalent Plexiglas plates, the palm facing down and the fingers semiflexed to mimic the natural posture of the hand.

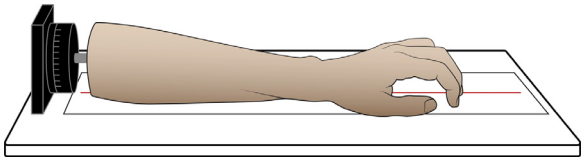

Fig. 3. Set-up for rotation measurements. The forearm was frozen to maintain the wrist in slight extension and fingers semiflexed during rotation, mimicking the posture of the patients´ forearm.

arthroplasty and scan mode nine double examinations were made by comparing the first and second scan, second, and third scan, and so on. To test the effect of thawing on BMD 5 scans with Motec were performed instantly after introducing the cadaver to room temperature, repeated after 1, 2, and 3 hours without moving (Fig. 2).

To assess the effect of forearm rotation on BMD, a screw inserted along the proximal diaphyseal radius axis during the first operation, was attached to the rotation stage of a micrometer with 0.1˚ increment (Thorslabs, Inc, Newton, NJ, USA), enabling rotation of the entire frozen forearm about the long axis of the radius (Fig. 3). From the completely pronated posture with the forearm lying flat on the table, 20˚ of supination (corresponding to a position with 70˚ pronation) was accomplished at increments of 5˚. Ten femur mode scans were performed at each position with Motec. Pronation exceeding 90˚ cannot be expected and was not measured.

To allow unrestricted wrist movement the cadaver was thawed at room temperature for 12 hours (Fig. 4). A protractor with 1˚ increments placed on the dorsal side of the wrist was used to measure the angle between the forearm and hand. Ten femur mode scans were performed at 0˚ and every 5˚ increment of extension up to 20˚ with the Motec implant. Wrist flexion cannot be expected during scanning of patients and was not measured.

Patient Double Examinations

Forty patients participating in a prospective, randomized clinical trial comparing the 2 arthroplasties (ClinicalTrials.gov NCT01842724), 20 in each group, gave written informed consent and underwent double DXA examinations on femur mode convertible to orthopedic knee

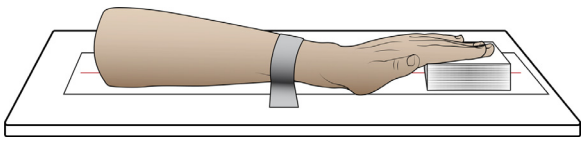

Fig. 4. Set-up for extension measurements. The forearm was secured to two plexiglas plates with duct tape a few cm proximal to the wrist, allowing free extension of the hand. Layers of paper underneath the fingers secured the hand in each position.

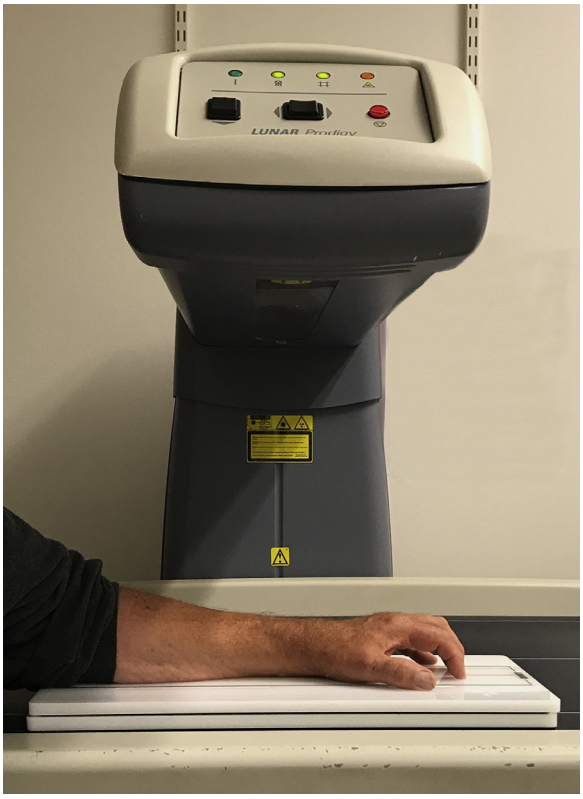

Fig. 5. DXA examination of patient sitting with the forearm pronated on the table. The hand was in a relaxed position with the fingers semiflexed. This was the most suitable position since many patients experienced discomfort on stretching out the fingers postoperatively.

mode 3 months postoperatively by standing up and repositioning the arm between the examinations. The study was approved by the regional ethics committee (ref. nr: 2013/149). The mean age and male:female ratio for patients with Motec and ReMotion TWA were 57 (SD 8, range 40–70) and 57 (SD 8, range 31–70) years and 14:6 and 18:2, respectively. The set-up was equivalent to the cadaver study with identical tissue plates, striving for indistinguishable arm/hand positioning (Fig. 5).

DXA Scans

A narrow fan beam (GE Healthcare Lunar Prodigy advance, Lunar Corp. Madison WI, USA) densitometer was used. Scans were performed with the femur and forearm modes of the enCORE software version 14.10 from GE Healthcare. Femur scan mode option “thin” was used, meaning that the tissue thickness was never expected to exceed 13 cm. The 20 cm long and 17 cm wide scan window started at the proximal phalanges, terminating 4–6 cm proximal to the radial implant. Average scanning time was 49 seconds and the radiation dose 9.0 μGy. The forearm mode scan window was 14 cm long and

10 cm wide, starting at the metacarpophalangeal joints and terminating 1.5–2.5 cm proximal to the radial implant. Average scanning time was 21 seconds and the radiation dose 2.0 μGy. Scanning resolution was 0.60×1.05 mm for both modes. Right position for ROI delineation was used. BMD was presented in grams of mineral per square centimeter (g/cm^2).

Analysis

Since the DXA scanner lacked the orthopedic software, all femur mode scans were converted to orthopedic knee mode on a separate computer using the orthopedic enCORE v16 software platform (GE Healthcare). The dynamic edge detection algorithm of the software automatically separated bone from soft tissue, air and artefact, and outlined a neutral area along the border between bone and soft tissue. The implant was detected as artefact and automatically removed from the BMD analysis. Inaccurate edge detection of varying degrees was noted on most scans, demanding manual correction. The time required for manual correction of the cadaver scans with implants was noted. The later removed lunate, triquetrum, and two-third of scaphoid were point-typed as neutral and eliminated from the cadaver scans obtained prior to implant insertion to include identical bones in all scans.

Regions of Interest

We defined 1 ROI around the distal components. Along the proximal components we defined 2 different models with 1 and 3 ROIs. All ROIs were rectangular (Fig. 6).

ROI templates were created for the cadaver scans, and copied to all other scans with the same implant, using the bony edges outlined in the enCORE software as reference. ROIs were copied from one scan with Motec implant and one scan with ReMotion implant to all scans without implant. To make the position of the ROIs as similar as possible on scans with and without implants, the third carpometacarpal joint was used as landmark for placing the distal ReMotion ROI, the proximal end of the capitate and the third metacarpophalangeal joint when present as landmark for the distal Motec ROI, and the radial styloid as landmark for all other ROIs. In each patient ROIs from the postoperative scan were copied to all later scans. Since the length of the 2 implants differed, the height and position of corresponding ROIs also differed. The difference in length and distance between the center of corresponding ROIs in the proximal to distal direction were calculated on cadaver scans.

Statistics

IBM SPSS Statistics version 26 (IBM Co., Armonk, NY, USA) was used for statistical analysis.

Normality was assumed if histograms were bell shaped. BMD, area, time and differences investigated with t-test were presented as bootstrapped means and 95% confidence intervals (CI) based on 1000 replications.

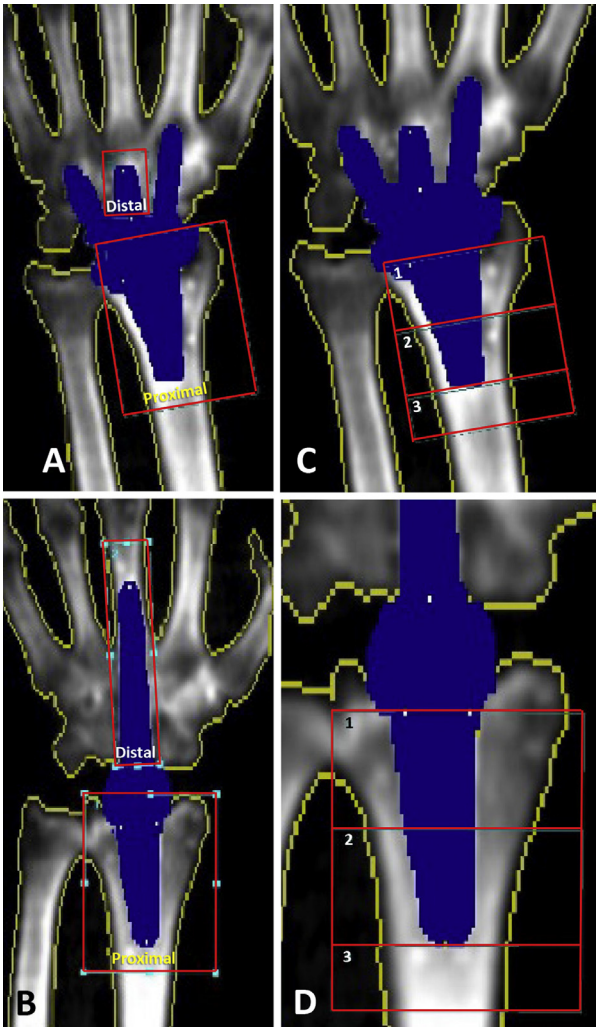

Fig. 6. (**A**–**D**). Regions of interest (ROI). One ROI around the distal implants. Two lines run parallel with the long axis of the third metacarpal, crossing the intersections between the second and third, and the third and fourth metacarpals, respectively. The ROI is limited by the proximal end of the capitate, and distally by a distance from the implant tip equaling one-fourth of the stem length (A, B). Only the capitate is included for ReMotion (A) whereas for Motec the entire length of the capitate and a large proportion of the third metacarpal is contained (B). One ROI along the proximal implant. Two lines run parallel with the long axis of the radius. The ulnar line passes through the distal radioulnar joint (DRUJ). Distally the ROI is limited by the end of the radial styloid, and proximally by a distance from the implant tip equaling one-fourth of the stem length (A-B). Three ROIs around the proximal implant. The distance from the tip to the most distal point of the stem defines 2 ROIs with equal height, ROI 1 and 2. ROI 3 extends 1 cm proximal to the implant tip (C, D).

Table 1
BMD Difference (Δ BMD) Between Motec and ReMotion ROIs in the Frozen Cadaver Before and After Inserting the Implants (n = 10; Mean, 95% CI). Scans with ReMotion Subtracted From Scans With Motec

ROI	Δ ROI height (cm)	Δ ROI center (cm)	Forearm mode		Ortho knee mode	
			Δ BMD without implant (g/cm^2)	Δ BMD with implant (g/cm^2)	Δ BMD without implant (g/cm^2)	Δ BMD with implant (g/cm^2)
Distal	3.90	1.95	0.004 (−0.002, 0.010)	0.102 (0.089, 0.114)*	0.034 (0.031, 0.037)*	0.093 (0.075, 0.113)*
Proximal	1.90	0.85	0.034 (0.031, 0.036)*	0.021 (0.008, 0.033)*	0.027 (0.026, 0.028)*	0.021 (0.017, 0.026)*
1	0.40	0.20	−0.013 (−0.021, −0.004)*	0.045 (0.034, 0.058)*	−0.034 (−0.036, −0.032)*	0.058 (0.052, 0.066)*
2	0.40	0.60	0.106 (0.099, 0.112)*	0.037 (0.020, 0.051)*	0.087 (0.082, 0.092)*	0.014 (0.006, 0.022)*
3	0	0.80	0.048 (0.033, 0.065)*	0.074 (0.050, 0.098)*	0.041 (0.035, 0.046)*	0.091 (0.086, 0.096)*

*$p < 0.05$.

Precision (repeatability) is usually presented as "coefficient of variation" (CV%) and "least significant change" (LSC%) in DXA studies. CV% was calculated using the following formula *(19)*, which is in accordance with the guidelines of The International Society of Densitometry (20):

$$CV\% = 100 \times \left(\frac{\sqrt{\Sigma (a-b)^2 / 2n}}{m} \right)$$

where a and b represent the BMD of the first and second measurement, n is the number of double examinations, and m the mean of all BMD measurements.

LSC% is the lowest measured BMD change in percent that cannot be explained by measurement error alone, and thus represents true BMD change in 95% of cases. LSC% was calculated as follows:

$$LSC\% = CV\% \times \sqrt{2} \times 1.96$$

Levene's test for equality of variances was used to compare precision between scan modes and implants. *p*Values < 0.05 were considered statistically significant.

Results

Table 1 shows the difference in height and longitudinal location of corresponding Motec and ReMotion ROIs. All Motec ROIs extended further from the joint than the corresponding ReMotion ROIs. BMD was higher in all Motec ROIs than the corresponding ReMotion ones with both modes on scans with implants ($p < 0.05$). On scans prior to implant insertion 3 of 5 Motec ROIs exhibited higher BMD than the corresponding ReMotion ROIs with forearm mode, and in 4 ROIs with orthopedic knee mode ($p < 0.05$; Table 1).

BMD changed with 10° of cadaver forearm supination in the distal ROI and ROI 1, and with 15° supination in the proximal ROI and ROI 2 ($p < 0.05$; Table 2). In the distal ROI, BMD increased with the first 5° of extension ($p < 0.05$). No other ROIs were affected by wrist extension up to 20° (Table 3). BMD decreased in the distal ROI from zero to 2 hours and 3 hours of thawing in all other ROIs ($p < 0.05$; Table 4).

Table 2
BMD Change (Δ BMD) With Supination From the Complete Pronated Position for Motec in the Frozen Cadaver (n = 10; Mean, 95% CI). Data at Pronation Subtracted From Data With Various Degrees of Supination

ROI	Neutral BMD(g/cm^2)	5° Δ BMD(g/cm^2)	10° Δ BMD(g/cm^2)	15° Δ BMD(g/cm^2)	20° Δ BMD(g/cm^2)
Distal	0.566 (0.560, 0.571)	0.003 (−0.014, 0.011)	−0.013 (−0.023, −0.003)*	−0.033 (−0.046, −0.021)*	−0.004 (−0.014, 0.007)
Proximal	0.612 (0.611, 0.613)	0.002 (−0.002, 0.006)	−0.002 (−0.006, 0.002)	−0.035 (−0.040, −0.030)*	−0.042 (−0.054, −0.030)*
1	0.548 (0.545, 0.553)	−0.005 (−0.012, 0.003)	−0.023 (−0.045, −0.008)*	−0.043 (−0.047, −0.039)*	−0.064 (−0.074, −0.053)*
2	0.658 (0.650, 0.664)	0.009 (−0.001, 0.016)	−0.005 (−0.012, 0.002)	−0.034 (−0.046, −0.023)*	−0.042 (−0.054, −0.025)*
3	0.758 (0.755, 0.760)	−0.001 (−0.003, 0.002)	0.004 (−0.001, 0.009)	−0.007 (−0.016, 0.001)	0.002 (−0.004, 0.009)

*$p < 0.05$.

Table 3
BMD Change (Δ BMD) With Wrist Extension for Motec in the Thawed Cadaver (n = 10; Mean, 95%CI). Data at the Neutral Position Subtracted From Data With Wrist Extension

ROI	Neutral BMD (g/cm^2)	5° Δ BMD (g/cm^2)	10° Δ BMD (g/cm^2)	15° Δ BMD (g/cm^2)	20° Δ BMD (g/cm^2)
Distal	0.498 (0.490, 0.507)	0.014 (0.003, 0.024)*	0.026 (0.008, 0.040)*	0.048 (0.035, 0.062)*	0.056 (0.040, 0.074)*
Proximal	0.572 (0.565, 0.580)	0.005 (−0.005, 0.014)	0.006 (−0.006, 0.01)	0.008 (−0.001, 0.01)	0.007 (−0.002, 0.015)
1	0.513 (0.503, 0.523)	−0.002 (−0.013, 0.009)	−0.005 (−0.019, 0.009)	0.004 (−0.006, 0.014)	0.006 (−0.005, 0.018)
2	0.620 (0.613, 0.628)	−0.002 (−0.014, 0.008)	0.000 (−0.014, 0.013)	0.009 (−0.004, 0.023)	−0.004 (−0.023, 0.011)
3	0.715 (0.702, 0.728)	0.003 (−0.011, 0.016)	0.005 (−0.017, 0.027)	0.009 (−0.006, 0.024)	0.009 (−0.007, 0.024)

*$p < 0.05$.

The mean time required for correcting the cadaver scans was shorter with orthopedic knee mode (5.3 [95% CI: 4.8, 5.9] minutes) than with forearm mode (11.0 [95%CI: 10.7, 11.4] minutes; $p < 0.05$).

Table 5 demonstrates the precision of the cadaver study comparing the 2 modes. The proximal ROI, and ROI 2 and 3 around the Motec revealed a significantly better precision with the orthopedic knee mode than with the forearm mode ($p < 0.05$).

In the clinical study the CV with the orthopedic knee mode ranged from 2.21% to 3.08% for the distal ROI, 1.66%−2.01% for the proximal ROI, and 1.98%−2.87% with 3 ROIs (Table 6). Neither precision nor BMD differed significantly between the 2 implants in any ROI ($p > 0.05$).

Discussion

The higher BMD in Motec than corresponding ReMotion ROIs in the cadaver can be explained by the different implant lengths. The Motec ROIs reach more proximally in the radius where BMD is higher *(21)* than the shorter ReMotion ROIs. The same applies to hip stems with uneven length where BMD doubles or more from proximal to distal *(12,22)*. Consequently, in comparative DXA studies BMD change and not absolute BMD values should be reported. The BMD change should be reported as absolute change and not percentage change, since implants with high BMD require higher absolute BMD change to reach the same percentage change as implants with lower BMD.

Table 4
BMD Change (Δ BMD) for Motec Following Thawing of the Cadaver (n = 5; Mean, 95%CI). Data at 0 Hour Subtracted From Data at Later Hours

ROI	0h BMD (g/cm^2)	1h Δ BMD (g/cm^2)	2h Δ BMD (g/cm^2)	3h Δ BMD (g/cm^2)
Distal	0.567 (0.559, 0.575)	−0.002 (−0.005, 0.002)	−0.020 (−0.030, −0.010)*	−0.064 (−0.069, −0.058)*
Proximal	0.611 (0.608, 0.614)	−0.004 (−0.012, 0.000)	0.001 (−0.005, 0.004)	−0.032 (−0.039, −0.025)*
1	0.549 (0.543, 0.555)	−0.007 (−0.017, 0.003)	−0.003 (−0.008, 0.003)	−0.035 (−0.055, −0.025)*
2	0.661 (0.655, 0.667)	0.005 (−0.001, 0.014)	0.004 (−0.02, 0.010)	−0.045 (−0.061, −0.026)*
3	0.756 (0.747, 0.762)	−0.006 (−0.015, 0.002)	0.000 (−0.009, 0.009)	−0.018 (−0.026, −0.010)*

*$p < 0.05$.

Table 5
Precision for Motec and ReMotion in the Cadaver Study Comparing the Forearm and Orthopedic Knee Modes (n = 9 Double Examinations)

ROI	Implant	Forearm mode			Ortho knee mode		
		Area (cm^2)	CV%	LSC%	Area (cm^2)	CV%	LSC%
Distal	Motec	2.81 (2.72, 2.90)	3.01	8.33	2.99 (2.74, 3.30)	1.76[a]	4.89[a]
	ReMotion	1.39 (1.30, 1.49)	3.41	9.45	1.45 (1.41, 1.48)	2.84	7.87
Proximal	Motec	5.95 (5.82, 6.08)	2.79[b]	7.73[b]	6.32 (6.19, 6.44)	0.73[b]	2.03[b]
	ReMotion	4.59 (4.42, 4.76)	2.24	6.20	4.78 (4.27, 5.04)	1.78[a]	4.94[a]
1	Motec	2.21 (2.13, 2.27)	1.77	4.90	2.18 (2.10, 2.25)	1.23[a]	3.40[a]
	ReMotion	1.75 (1.69, 1.82)	3.81	10.55	1.67 (1.65, 1.70)	1.53	4.24
2	Motec	1.50 (1.42, 1.56)	2.90[b]	8.03[b]	1.65 (1.61, 1.69)	1.35[b]	3.74[b]
	ReMotion	1.50 (1.41, 1.58)	2.29	6.35	1.72 (1.69, 1.75)	3.07[a]	8.50[a]
3	Motec	1.42 (1.36, 1.46)	5.67[b]	15.71[b]	1.58 (1.55, 1.60)	0.96[b]	2.66[b]
	ReMotion	1.67 (1.64, 1.69)	1.59[a]	4.40[a]	1.77 (1.75, 1.79)	1.48	4.09

[a]Histogram implying not normally distributed.
[b]Statistical difference in precision between forearm and orthopedic knee mode (Levene's test for equality of variances, $p < 0.05$).

The time required for correcting the orthopedic knee mode scans was less than half compared to the forearm mode scans, reflecting the more accurate edge detection with the orthopedic knee mode. The accuracy of edge detection affects the precision. In the proximal ROI, and ROI 2 and 3 around the Motec the precision was significantly better with the orthopedic knee mode than the forearm mode. We therefore recommend the orthopedic knee mode for BMD analysis of TWA.

BMD has been shown to decrease in 24 hours thawed cadaver femora *(16)*. In our study 1 hour thawing, which was the maximum time of any scanning session, did not affect BMD.

The measured BMD changed with 10° forearm rotation. The same has been shown with 5° rotation of a proximal tibial implant *(15)*. In our study only ROI 3 which is situated proximal to the implant tip was unaffected by 20° rotation. In that area the radius is nearly cylindrical, and the projection does not change much with rotation as opposed to the oval metaphysis. Therefore, during rotation BMD remains almost unchanged in ROI 3. Whether the same is true for the ReMotion is uncertain, since the center of ROI 3 was placed 0.8 cm more distally in the radius than the Motec. The true axis of forearm rotation runs from the radius head to the distal ulna and not along the longitudinal axis of the radius as in our model *(23)*. Thus, during forearm supination the radius not only rotates, but to some extent also moves in extension and ulnar translation. We therefore expect that forearm rotation affects BMD to a larger extent than our cadaver study reveals.

Whereas the proximal component ROIs were unaffected by 20° wrist extension, the BMD in the distal ROI changed with only 5° extension, similar to a tibial implant in which BMD changed with 5° knee flexion *(24)*. As the wrist extends and the angle between the x-ray beam and the longitudinal axis of the hand decreases, the projected bone area also decreases, whereas the bone mineral content remains the same, resulting in increased BMD. In our study the forearm was lying flat on the scan table whereas the fingers were somewhat flexed. Changing the degree of finger flexion changes the angle of the wrist as long as the forearm remains flat on the scan table. Since 5° wrist extension results from a quite small movement of the fingers, combined with the fact that we did not have any means to control the finger position on subsequent scans, we conclude that the longitudinal precision with our study set-up is probably too poor to allow BMD measurement of the distal ROI. We made the first DXA scan 2–3 days postoperatively, at a time many patients

Table 6
BMD (Mean, 95% CI) and Precision in the Clinical Study Comparing Motec and ReMotion (n = 20 Double Examinations)

ROI	Implant	Area (cm^2)	BMD (g/cm^2)	CV%	LSC%
Distal	Motec	3.05 (2.70, 3.38)	0.423 (0.392, 0.453)	2.21	6.11
	ReMotion	0.98 (0.90, 1.06)	0.448 (0.389, 0.504)	3.08	8.52
Proximal	Motec	8.08 (7.48, 8.65)	0.506 (0.471, 0.541)	1.66	4.59
	ReMotion	5.48 (5.00, 5.96)	0.478 (0.436, 0.518)	2.01	5.56
1	Motec	3.20 (2.93, 3.44)	0.426 (0.390, 0.463)	2.54	7.05
	ReMotion	2.03 (1.86, 2.17)	0.378 (0.328, 0.428)	2.70	7.49
2	Motec	2.18 (2.00, 2.36)	0.558 (0.515, 0.596)	2.12	5.88
	ReMotion	1.97 (1.79, 2.15)	0.514 (0.473, 0.552)	2.87	7.96
3	Motec	1.77 (1.67, 1.86)	0.685 (0.635, 0.731)	2.06	5.49
	ReMotion	1.82 (1.71, 1.92)	0.622 (0.575, 0.665)	1.98	5.43

experienced discomfort on stretching the fingers. By postponing the first scan 1 or 2 weeks it should be possible to scan all patients with the palm and fingers flat on the table, controlling for both wrist extension and forearm rotation, thereby improving the precision.

Precision was calculated from double examinations. Whereas the patients were repositioned to mimic the longitudinal precision, the cadaver forearm was not. The precision of BMD analysis in the forearm is affected by the consistency of tissue labeling *(25)* and ROI placement on successive scans *(21)*. In addition, the consistency of joint alignment in rotation and flexion-extension affects the precision of BMD measurement around total hip arthroplasties *(12,26)* and knee arthroplasties *(15,24,27)*. The precision in the cadaver was therefore probably false high. The clinical precision with our 3 ROI model was equal to or higher than a 2 and 3 ROI model used in a total ankle arthroplasty with CVs ranging from 1.48% to 4.89% *(28)*. The highest precision in the ankle was found in a calcaneal ROI which was larger than the other ROIs, and did not include the prosthesis, thereby omitting any inaccuracy of point typing the implant to bone interface. Our 3 ROI precision was equal to a proximal tibial 3 ROI model when correcting for the different ways of calculating precision *(15,24)*. As in our study the highest precision was found in the ROI situated underneath the stem, probably due to the smaller area of implant bone interface than the other ROIs *(15,24)*. Precision in the wrist was also similar to a 6 ROI model of a distal femoral implant *(27)*, a 1 and 2 ROI hip resurfacing model, and higher than a 6 ROI hip resurfacing model *(29)*. Our 3 ROI precision was equal to or higher than a 3 and 4 ROI acetabular model *(13,14)*, but not as high as the 7 ROI model of the hip *(13)*.

The higher precision in the hip as compared to the wrist may be due to better control of alignment of the extremity by using a foot brace during scanning, combined with larger sized ROIs. The specific orthopedic hip software probably contributes to more accurate tissue detection in the hip.

In conclusion, DXA is feasible for BMD measurement around a proximal wrist implant using the orthopedic knee mode and a 3 ROI model. With the available software and our study set-up DXA is unsuitable for distal implant measurement. Since DXA is sensitive to forearm rotation and wrist extension, the position of the forearm during scanning should be standardized. BMD differs between implants of unequal length. Therefore, BMD change and not absolute BMD should be reported in comparative DXA studies.

Acknowledgments

The authors thank Øystein H Horgmo (engineer; Medical Photography and Illustration Service, Institute of Clinical Medicine, University of Oslo) for help with illustrations, and Lien My Diep (statistician; Oslo Centre for

Biostatistics and Epidemiology, Oslo University Hospital) for help with statistics.

References

1. Reigstad O, Rokkum M. 2014 Wrist arthroplasty: where do we stand today? A review of historic and contemporary designs. Hand Surg 19:311–322.
2. Yeoh D, Tourret L. 2015 Total wrist arthroplasty: a systematic review of the evidence from the last 5 years. J Hand Surg Eur Vol 40:458–468.
3. Boeckstyns ME, Herzberg G, Merser S. 2013 Favorable results after total wrist arthroplasty: 65 wrists in 60 patients followed for 5-9 years. Acta Orthop 84:415–419.
4. Reigstad O, Holm-Glad T, Bolstad B, et al. 2017 Five- to 10-year prospective follow-up of wrist arthroplasty in 56 nonrheumatoid patients. J Hand Surg Am 42:788–796.
5. Brodner W, Bitzan P, Lomoschitz F, et al. 2004 Changes in bone mineral density in the proximal femur after cementless total hip arthroplasty. A five-year longitudinal study. J Bone Joint Surg Br 86:20–26.
6. Parchi PD, Cervi V, Piolanti N, et al. 2014 Densitometric evaluation of periprosthetic bone remodeling. Clin Cases Miner Bone Metab 11:226–231.
7. Venesmaa P, Kroger H, Miettinen H, et al. 2000 Bone loss around failed femoral implant measured by dual-energy X-ray absorptiometry. J Orthop Sci 5:380–384.
8. Wilkinson JM, Hamer AJ, Rogers A, et al. 2003 Bone mineral density and biochemical markers of bone turnover in aseptic loosening after total hip arthroplasty. J Orthop Res 21:691–696.
9. Laursen MB, Nielsen PT, Soballe K. 2006 Detection of bony defects around cementless acetabular components in total hip arthroplasty: a DEXA study on 10 human cadavers. Acta Orthop 77:209–217.
10. Yan SG, Weber P, Steinbruck A, et al. 2018 Periprosthetic bone remodelling of short-stem total hip arthroplasty: a systematic review. Int Orthop 42:2077–2086.
11. Gehrchen PM, Petersen MM, Nielsen PK, Lund B. 2000 Influence of region size on bone mineral measurements along femoral stems in THA. HIP Int 10:204–208.
12. Kroger H, Miettinen H, Arnala I, et al. 1996 Evaluation of periprosthetic bone using dual-energy x-ray absorptiometry: precision of the method and effect of operation on bone mineral density. J Bone Miner Res 11:1526–1530.
13. Lindalen E, Dahl J, Nordsletten L, et al. 2012 Reverse hybrid and cemented hip replacement compared using radiostereometry and dual-energy X-ray absorptiometry: 43 hips followed for 2 years in a prospective trial. Acta Orthop 83:592–598.
14. Wilkinson JM, Peel NF, Elson RA, et al. 2001 Measuring bone mineral density of the pelvis and proximal femur after total hip arthroplasty. J Bone Joint Surg Br 83: 283-238.
15. Tjornild M, Soballe K, Bender T, Stilling M. 2011 Reproducibility of BMD measurements in the prosthetic knee comparing knee-specific software to traditional DXA software: a clinical validation. J Clin Densitom 14:138–148.
16. Wahnert D, Hoffmeier KL, Lehmann G, et al. 2009 Temperature influence on DXA measurements: bone mineral density acquisition in frozen and thawed human femora. BMC Musculoskelet Disord 10:25.
17. Gupta A. 2008 Total wrist arthroplasty. Am J Orthop (Belle Mead NJ) 37:12–16.
18. Reigstad A, Reigstad O, Grimsgaard C, Rokkum M. 2011 New concept for total wrist replacement. J Plast Surg Hand Surg 45:148–156.
19. El Maghraoui A, Achemlal L, Bezza A. 2006 Monitoring of dual-energy X-ray absorptiometry measurement in clinical practice. J Clin Densitom 9:281–286.
20. Schousboe JT, Shepherd JA, Bilezikian JP, Baim S. 2013 Executive summary of the 2013 international society for clinical densitometry position development conference on bone densitometry. J Clin Densitom 16:455–466.
21. Rosen EO, McNamara EA, Whittaker LG, et al. 2018 Effect of positioning of the ROI on BMD of the forearm and its subregions. J Clin Densitom 21:529–533.
22. Freitag T, Hein MA, Wernerus D, et al. 2016 Bone remodelling after femoral short stem implantation in total hip arthroplasty: 1-year results from a randomized DEXA study. Arch Orthop Trauma Surg 136:125–130.
23. Kiratli BJ, Heiner JP, McBeath AA, Wilson MA. 1992 Determination of bone mineral density by dual x-ray absorptiometry in patients with uncemented total hip arthroplasty. J Orthop Res 10:836–844.
24. Stilling M, Soballe K, Larsen K, et al. 2010 Knee flexion influences periprosthetic BMD measurement in the tibia. Suggestions for a reproducible clinical scan protocol. Acta Orthop 81:463–470.
25. Krueger D, Vallarta-Ast N, Libber J, et al. 2013 Positioner and clothing artifact can affect one-third radius bone mineral density measurement. J Clin Densitom 16:154–159.
26. Mortimer ES, Rosenthall L, Paterson I, Bobyn JD. 1996 Effect of rotation on periprosthetic bone mineral measurements in a hip phantom. Clin Orthop Relat Res 324:269–274.
27. Therbo M, Petersen MM, Schroder HM, et al. 2003 The precision and influence of rotation for measurements of bone mineral density of the distal femur following total knee arthroplasty: a methodological study using DEXA. Acta Orthop Scand 74:677–682.
28. Messina C, Usuelli FG, Maccario C, et al. 2019 Precision of bone mineral density measurements around total ankle replacement using dual energy X-ray absorptiometry. J Clin Densitom doi:10.1016/j.jocd.2019.01.006.
29. Penny JO, Ovesen O, Brixen K, et al. 2010 Bone mineral density of the femoral neck in resurfacing hip arthroplasty. Acta Orthop 81:318–323.